Computing 68, 313–341 (2002)
Digital Object Identifier (DOI) 10.1007/s00607-002-1444-2

Computing
Printed in Austria

Non-Nested Multi-Level Solvers for Finite Element Discretisations of Mixed Problems

V. John, Magdeburg, **P. Knobloch,** Praha, **G. Matthies** and **L. Tobiska,** Magdeburg

Received May 17, 2001; revised February 2, 2002
Published online April 25, 2002

Abstract

We consider a general framework for analysing the convergence of multi-grid solvers applied to finite element discretisations of mixed problems, both of conforming and nonconforming type. As a basic new feature, our approach allows to use different finite element discretisations on each level of the multi-grid hierarchy. Thus, in our multi-level approach, accurate higher order finite element discretisations can be combined with fast multi-level solvers based on lower order (nonconforming) finite element discretisations. This leads to the design of efficient multi-level solvers for higher order finite element discretisations.

AMS Subject Classifications: 65N55, 65N30, 76D07.

Keywords: Multi-level method, finite element discretisation, mixed problems, Stokes problem.

1. Introduction

Multi-grid methods are among the most efficient and most popular solvers for finite element discretisations of elliptic partial differential equations. Their convergence theory in the case of symmetric operators and nested conforming finite element methods is well-established; see for example the books [7, 18, 32] and the bibliographies therein. Multi-grid methods for nonconforming finite element approximations have been also studied in a number of papers, e.g. see [3, 4, 6, 8–14, 21, 33]. In this case, the finite element space of a coarser level is in general not a subspace of the finite element space of a finer level; the resulting multi-grid method is called non-nested. The general framework of analysing the two-level convergence of non-nested multi-grid methods, developed in [4] for elliptic problems, will be the starting point for the methods studied herein. Multi-grid methods for mixed problems, arising in the discretisation of the Stokes equations, are analysed in [3, 5, 9, 21, 29, 33, 36]. The crucial point in the investigation of multi-grid methods for mixed problems is the definition and analysis of the smoother. The currently best understood type of smoothers, here called Braess–Sarazin type smoother, is a class of symmetric incomplete Uzawa iterations proposed in [1] and analysed on its smoothing properties in [5, 29, 36]. The Braess–Sarazin type smoother has a convergence rate of $\mathcal{O}(1/m)$ with respect to

the number of smoothing steps m. By far, most of the analytical studies are applied to standard multi-grid methods where on each multi-grid level the same discretisation of the partial differential equation is used.

In this paper, we investigate multi-level solvers for finite element discretisations of mixed problems which allow different discretisations, in particular the use of different finite element spaces, on each level of the multi-grid hierarchy. The motivation for using this type of multi-level solvers comes from general experiences that standard multi-level solvers are very efficient for low order discretisations. But higher order discretisations might lead to an overwhelming gain of accuracy of the computed solution so that their use should be preferred for this reason. The multi-level solvers investigated in this paper allow an accurate discretisation on the finest level and low order discretisations on all coarser levels. In this way, an accurate solution can be obtained for whose computation the efficiency of multi-level solvers for low order discretisations is exploited. The crucial point in the construction of such multi-level methods is the transfer operator between the finite element spaces defined on different levels. We show that rather simple L^2-stable prolongations guarantee already the convergence of the two-level method for a sufficiently large number of smoothing steps with a Braess–Sarazin type smoother. Our approach allows to handle conforming and nonconforming finite element spaces in a general framework. As a concrete application of the general theory developed in this paper, we have in mind in particular the Stokes and Navier–Stokes equations. The efficiency of multi-grid solvers for lowest order nonconforming discretisations of these equations has been demonstrated, e.g., in [22, 34] and the gain of accuracy of higher order discretisations in a benchmark problem in [19, 20]. Let us mention that the ideas presented in this paper can be also applied to selfadjoint elliptic equations.

Different discretisations on the finest and on coarser grids have been already used in the convergence theory of nonconforming finite element discretisations of the Poisson equation in [13, 14]. However, the motive of the approach in [13, 14] is completely different to ours. The replacement of the P_1-nonconforming coarse grid correction by a conforming P_1 coarse grid correction enables the authors to apply the well-developed theory of multi-grid solvers for conforming discretisations on the coarser levels.

The plan of the paper is as follows. In Section 2, we investigate the convergence properties of a multi-level method for solving mixed finite element discretisations in an abstract way. First, we introduce the variational and the discrete mixed problem and we describe the matrix representation. Then, based on abstract mappings between finite element spaces, the prolongation and restriction operators are defined. As the smoother we use the basic iteration proposed in [5], for which the smoothing property has been shown in [5, 29, 36] in case of symmetric positive definite spectral equivalent pre-conditioners. Together with the approximation property, the convergence of a two-level method and the W-cycle of a multi-level method is established. Section 3 is devoted to the construction of a general mapping between two finite element spaces. We show that this general transfer operator satisfies all assumptions which are essential for our theory. As

applications, we show in Section 4 how various discretisation concepts for solving the Stokes problem fit in our general theory. Finally, we present numerical results to verify the theoretical predictions on the multi-level solvers.

Throughout this paper, we denote by C a "universal" constant which is independent of the mesh size and the level but whose value can differ from place to place.

2. Multi-Level Approach

2.1. Variational Problem

We consider a variational problem of the following form. Let V and Q be two Hilbert spaces and let $V \subset H \subset V'$ be the Gelfand triple. Given the symmetric bilinear form $a : V \times V \to \mathbb{R}$, the bilinear form $b : V \times Q \to \mathbb{R}$ and a functional $f \in V'$, we look for a solution $(u, p) \in V \times Q$ of

$$a(u, v) + b(v, p) = f(v) \quad \forall\, v \in V, \tag{1}$$

$$b(u, q) = 0 \quad \forall\, q \in Q. \tag{2}$$

We assume:

(H1) (Solvability) For all $f \in V'$, the problem (1), (2) admits a unique solution $(u, p) \in V \times Q$ with

$$\|u\|_V + \|p\|_Q \leq C\|f\|_{V'}.$$

One example for this type of problems is the weak formulation of the Stokes problem in d space dimensions ($d = 2, 3$)

$$\begin{aligned} -\Delta u + \nabla p &= f \quad \text{in } \Omega \subset \mathbb{R}^d, \\ \nabla \cdot u &= 0 \quad \text{in } \Omega, \\ u &= 0 \quad \text{on } \partial\Omega, \end{aligned} \tag{3}$$

where Ω is a bounded domain with Lipschitz continuous boundary. Here we set $V = H_0^1(\Omega)^d$, $Q = L_0^2(\Omega)$, $H = L^2(\Omega)^d$, and a and b are given by

$$a(u, v) = \int_\Omega \nabla u : \nabla v \, dx, \quad b(v, p) = -\int_\Omega p \nabla \cdot v \, dx. \tag{4}$$

Note that in this case (H1) is satisfied [17] since a is V-elliptic and b satisfies the Babuška–Brezzi condition, i.e., there is a positive constant β such that

$$\sup_{v \in V} \frac{b(v, q)}{\|v\|_V} \geq \beta \|q\|_Q \quad \forall\, q \in Q. \tag{5}$$

2.2. Discretisation

Let $V_l \subset H$ and $Q_l \subset Q$, $l = 0, 1, \ldots$, be sequences of (possibly nonconforming) finite element spaces approximating V and Q, respectively. Instead of the continuous bilinear forms a and b we use the discrete versions $a_l : V_l \times V_l \to \mathbb{R}$ and $b_l : V_l \times Q_l \to \mathbb{R}$, respectively. We again assume that the bilinear forms a_l are symmetric. For $f \in H$ the discrete problem corresponding to (1), (2) reads

Find $(u_l, p_l) \in V_l \times Q_l$ such that

$$a_l(u_l, v_l) + b_l(v_l, p_l) = (f, v_l) \quad \forall\, v_l \in V_l, \tag{6}$$

$$b_l(u_l, q_l) = 0 \quad \forall\, q_l \in Q_l, \tag{7}$$

where $(\cdot, \cdot)$ denotes the inner product in H.

(H2) (Solvability and convergence) We assume that the problem (6), (7) admits a unique solution and that the error estimate

$$\|u - u_l\|_H \leq C h_l^2 \|f\|_H \tag{8}$$

holds, where h_l characterises how fine is the finite element mesh on which V_l and Q_l are defined.

Remark 2.1. *Typically, the convergence estimate* (8) *is established using a regularity property of the problem* (1), (2). *Such a regularity property usually states that if $f \in H$, then the solution (u, p) of* (1), (2) *belongs to a 'better' space $W \times R \subset V \times Q$ and satisfies*

$$\|u\|_W + \|p\|_R \leq C \|f\|_H.$$

For example, for the Stokes problem mentioned above, one has $W = (H^2(\Omega) \cap H_0^1(\Omega))^d$, $R = H^1(\Omega) \cap L_0^2(\Omega)$, and the regularity property holds if the boundary of Ω is of class C^2 or Ω is a plane convex polygon. For $(u, p) \in W \times R$ one can often prove that the solution of (6), (7) *satisfies*

$$\|u - u_l\|_H \leq C h_l^2 (\|u\|_W + \|p\|_R)$$

and taking into considerations the estimate in the regularity property, one obtains (8).

2.3. Matrix Representation

Let $\{\varphi_{l,i} : i \in I_l\}$ and $\{\psi_{l,j} : j \in J_l\}$ be bases of the spaces V_l and Q_l, respectively, where I_l, J_l denote the corresponding index sets. The unique representations

$$u_l = \sum_{i \in I_l} u_{l,i} \varphi_{l,i}, \quad p_l = \sum_{j \in J_l} p_{l,j} \psi_{l,j}$$

define the finite element isomorphisms $\Phi_l : \mathscr{U}_l \to V_l$, $\Psi_l : \mathscr{P}_l \to Q_l$ between the vector spaces $\mathscr{U}_l = \mathbb{R}^{\dim V_l}$, $\mathscr{P}_l = \mathbb{R}^{\dim Q_l}$ of coefficient vectors $\underline{u}_l = (u_{l,i})_{i \in I_l}$, $\underline{p}_l = (p_{l,j})_{j \in J_l}$ and the finite element spaces V_l and Q_l, respectively. We introduce the finite element matrices A_l and B_l having the entries $a_{l,ij} = a_l(\varphi_{l,j}, \varphi_{l,i})$ and $b_{l,ij} = b_l(\varphi_{l,j}, \psi_{l,i})$. Now the discrete problem (6), (7) is equivalent to

$$\begin{pmatrix} A_l & B_l^T \\ B_l & 0 \end{pmatrix} \begin{pmatrix} \underline{u}_l \\ \underline{p}_l \end{pmatrix} = \begin{pmatrix} \underline{f}_l \\ 0 \end{pmatrix} \tag{9}$$

with $f_{l,i} = (f, \varphi_{l,i})$. Note that A_l is a symmetric matrix. In the vector spaces $\mathscr{U}_l$ and $\mathscr{P}_l$, we will use the usual Euclidean norms scaled by suitable factors such that the following norm equivalences

$$\begin{aligned} C^{-1} \|\underline{v}_l\|_{\mathscr{U}_l} \leq \|v_l\|_H \leq C \|\underline{v}_l\|_{\mathscr{U}_l} \quad \forall\, v_l \in V_l, \\ C^{-1} \|\underline{q}_l\|_{\mathscr{P}_l} \leq \|q_l\|_Q \leq C \|\underline{q}_l\|_{\mathscr{P}_l} \quad \forall\, q_l \in Q_l, \end{aligned} \tag{10}$$

are satisfied with a mesh- and level-independent constant C.

2.4. Prolongation and Restriction

Essential ingredients of a multi-level algorithm for mixed problems are the prolongations

$$P_{l-1,l}^u : \mathscr{U}_{l-1} \to \mathscr{U}_l \,, \quad P_{l-1,l}^p : \mathscr{P}_{l-1} \to \mathscr{P}_l$$

and the restrictions

$$R_{l,l-1}^u := (P_{l-1,l}^u)^* : \mathscr{U}_l \to \mathscr{U}_{l-1} \,, \quad R_{l,l-1}^p := (P_{l-1,l}^p)^* : \mathscr{P}_l \to \mathscr{P}_{l-1}.$$

In case of a nested finite element hierarchy $V_0 \subset \cdots \subset V_{l-1} \subset V_l$, the canonical prolongation $P_{l-1,l}^u$ is obtained by the finite element isomorphisms between $\mathscr{U}_{l-1}$ and V_{l-1}, $\mathscr{U}_l$ and V_l and the embedding $V_{l-1} \subset V_l$, thus

$$P_{l-1,l}^u := \Phi_l^{-1} \circ \Phi_{l-1}.$$

Similarly, we would have

$$P_{l-1,l}^p := \Psi_l^{-1} \circ \Psi_{l-1}$$

for $Q_0 \subset \cdots \subset Q_{l-1} \subset Q_l$. The assumed inclusion property $Q_0 \subset \cdots \subset Q_{l-1} \subset Q_l$ is often but not always satisfied in applications. For example, this inclusion property is violated if the spaces Q_l are constructed using the nonconforming piecewise linear element. The corresponding velocity spaces V_l, such that the pair (V_l, Q_l) satisfies the discrete version of (5), may then be constructed using the bubble enriched nonconforming piecewise linear element [35] or the modified

nonconforming piecewise linear element [24]. As a different example one could also think of using a continuous pressure space Q_l on the level l and a discontinuous space Q_{l-1} on the level $l-1$. We emphasise that Q_{l-1} can be defined on the same mesh as Q_l.

In the general case of non-nested velocity spaces, when $V_{l-1} \not\subset V_l$, we have to replace the natural embedding by a suitable mapping $\iota_u : V_{l-1} \to V_l$, which results in the following prolongation and restriction:

$$P^u_{l-1,l} = \Phi_l^{-1} \circ \iota_u \circ \Phi_{l-1} \quad \text{and} \quad R^u_{l,l-1} = \Phi^*_{l-1} \circ \iota_u^* \circ (\Phi^*_l)^{-1}.$$

It turns out that the convergence analysis requires estimates for ι_u on the sum $V_{l-1} + V_l$, thus we will define $\iota_u : \Sigma_l \to V_l$ on the (possibly larger) space Σ_l with $V_{l-1} + V_l \subset \Sigma_l \subset H$. In the case $Q_{l-1} \not\subset Q_l$ we introduce a mapping $\iota_p : Q_{l-1} \to Q_l$ giving the following prolongation and restriction, respectively,

$$P^p_{l-1,l} = \Psi_l^{-1} \circ \iota_p \circ \Psi_{l-1} \quad \text{and} \quad R^p_{l,l-1} = \Psi^*_{l-1} \circ \iota_p^* \circ (\Psi^*_l)^{-1}.$$

We assume that the following properties of the mapping ι_u hold:

(H3) $\iota_u v = v \quad \forall\, v \in V_l$,

(H4) $\|\iota_u v\|_H \le C\|v\|_H \quad \forall v \in \Sigma_l$.

Remark 2.2. *In* [4], *the mapping ι_u has been assumed to be the product $\iota_u = \pi \circ \sigma$ with $\sigma : \Sigma_l \to S$ and $\pi : S \to V_l$ to allow more flexibility in constructing a suitable ι_u. In many cases S can be chosen to coincide with V_l or $\mathscr{U}_l$.*

2.5. Smoothing Property

For smoothing the error of an approximate solution of (9), we take the basic iteration

$$\begin{pmatrix} \alpha_l D_l & B_l^T \\ B_l & 0 \end{pmatrix} \begin{pmatrix} \underline{u}_l^{j+1} - \underline{u}_l^j \\ \underline{p}_l^{j+1} - \underline{p}_l^j \end{pmatrix} = \begin{pmatrix} \underline{f}_l \\ 0 \end{pmatrix} - \begin{pmatrix} A_l & B_l^T \\ B_l & 0 \end{pmatrix} \begin{pmatrix} \underline{u}_l^j \\ \underline{p}_l^j \end{pmatrix}, \tag{11}$$

$j \ge 0$, which can be considered as a special case of the symmetric incomplete Uzawa algorithm proposed by Bank, Welfert and Yserentant in [1]. The smoothing properties of (11) have been studied in [5] for the special case $D_l = I_l$, in [29] for the general case provided that an additional projection step is performed, and in [36] for a more general setting.

The matrix D_l is a pre-conditioner of A_l such that the linear system (11) is more easily solvable than (9). Note that we have

$$B_l(\underline{u}_l^{j+1} - \underline{u}_l^j) = -B_l \underline{u}_l^j, \quad j \ge 0,$$

implying that after one smoothing step the iterate $\underline{u}_l^{j+1}$, $j \geq 0$, is discretely divergence-free, i.e., $B_l \underline{u}_l^{j+1} = 0$. We assume that

(H5) D_l is symmetric and positive definite and $B_l B_l^T$ is non-singular.

The matrix $B_l B_l^T$ is non-singular if the bilinear form b_l, generating the matrix B_l satisfies a discrete version of the Babuška–Brezzi condition (5). Since $B_l B_l^T$ is non-singular, it follows that $S_l := B_l D_l^{-1} B_l^T$ is also non-singular and we have the representation

$$\begin{pmatrix} \alpha_l D_l & B_l^T \\ B_l & 0 \end{pmatrix}^{-1} = \begin{pmatrix} \frac{1}{\alpha_l}(I_l - D_l^{-1} B_l^T S_l^{-1} B_l) D_l^{-1} & D_l^{-1} B_l^T S_l^{-1} \\ S_l^{-1} B_l D_l^{-1} & -\alpha_l S_l^{-1} \end{pmatrix}.$$

It is easy to verify that

$$\begin{pmatrix} \underline{u}_l - \underline{u}_l^{j+1} \\ \underline{p}_l - \underline{p}_l^{j+1} \end{pmatrix} = \begin{pmatrix} \alpha_l D_l & B_l^T \\ B_l & 0 \end{pmatrix}^{-1} \begin{pmatrix} (\alpha_l D_l - A_l)(\underline{u}_l - \underline{u}_l^j) \\ 0 \end{pmatrix},$$

where $(\underline{u}_l, \underline{p}_l)$ is the solution of (9). This shows that the iteration is a so-called u-dominant method since the new iterate $(\underline{u}_l^{j+1}, \underline{p}_l^{j+1})$ depends on $\underline{u}^j$ but not on $\underline{p}^j$.

Lemma 2.1. *Let α_l be chosen such that*

$$\frac{1}{\delta} \lambda_{max}(A_l) < \alpha_l \lambda_{min}(D_l) \leq \alpha_l \|D_l\| \leq \gamma \lambda_{max}(A_l)$$

for some level- and mesh-independent constants $\delta \in [1, 2)$ and $\gamma > 0$. Moreover, let the basis $\{\varphi_{l,i} : i \in I_l\}$ be chosen such that $\lambda_{max}(A_l) = \mathcal{O}(h_l^{-2})$. Then, the basic iteration (11) *satisfies the smoothing property*

$$\|A_l(\underline{u}_l - \underline{u}_l^m) + B_l^T(\underline{p}_l - \underline{p}_l^m)\|_{\mathcal{U}_l} \leq \frac{C}{m} h_l^{-2} \|\underline{u}_l - \underline{u}_l^0\|_{\mathcal{U}_l}.$$

See [5, 29, 36]. □

2.6. Approximation Property

Let an approximation $(\tilde{\boldsymbol{u}}_l, \tilde{\boldsymbol{p}}_l) \in V_l \times Q_l$ of the solution $(u_l, p_l) \in V_l \times Q_l$ of the problem (6), (7) be given. We can think of $(\tilde{\boldsymbol{u}}_l, \tilde{\boldsymbol{p}}_l)$ as being the result after some smoothing steps, and consequently assume that

$$b_l(\tilde{\boldsymbol{u}}_l, q_l) = 0 \quad \forall\, q_l \in Q_l.$$

Then, the coarse-level correction is defined as the solution of the following problem:

Find $(u_{l-1}^*, p_{l-1}^*) \in V_{l-1} \times Q_{l-1}$ such that for all $(v_{l-1}, q_{l-1}) \in V_{l-1} \times Q_{l-1}$

$$a_{l-1}(u_{l-1}^*, v_{l-1}) + b_{l-1}(v_{l-1}, p_{l-1}^*) = (f, \iota_u v_{l-1}) - a_l(\tilde{\boldsymbol{u}}_l, \iota_u v_{l-1}) - b_l(\iota_u v_{l-1}, \tilde{\boldsymbol{p}}_l), \tag{12}$$

$$b_{l-1}(u_{l-1}^*, q_{l-1}) = 0. \tag{13}$$

The coarse-level correction yields via the transfer operators ι_u, ι_p from Section 2.4 the new approximation

$$u_l^{new} = \tilde{\boldsymbol{u}}_l + \iota_u u_{l-1}^*, \quad p_l^{new} = \tilde{\boldsymbol{p}}_l + \iota_p p_{l-1}^*.$$

Now, the basic idea for proving the approximation property is to construct an auxiliary (continuous) problem such that (u_{l-1}^*, p_{l-1}^*) and $(u_l - \tilde{\boldsymbol{u}}_l, p_l - \tilde{\boldsymbol{p}}_l)$ are finite element solutions of the corresponding discrete problems in the spaces $V_{l-1} \times Q_{l-1}$ and $V_l \times Q_l$, respectively. This idea has been used for scalar elliptic equations already in [6] and has been applied to more general situations in [4, 21]. We define the Riesz representation $F_l \in \Sigma_l$ of the residue by

$$(F_l, s) := (f, \iota_u s) - a_l(\tilde{\boldsymbol{u}}_l, \iota_u s) - b_l(\iota_u s, \tilde{\boldsymbol{p}}_l) \quad \forall\, s \in \Sigma_l.$$

Then, the auxiliary problem will be

Find $(z, w) \in V \times Q$ such that

$$\begin{aligned} a(z, v) + b(v, w) &= (F_l, v) \quad \forall\, v \in V, \\ b(z, q) &= 0 \quad \forall\, q \in Q. \end{aligned}$$

Indeed, for $s \in V_l$ we have

$$(F_l, s) = (f, s) - a_l(\tilde{\boldsymbol{u}}_l, s) - b_l(s, \tilde{\boldsymbol{p}}_l) = a_l(u_l - \tilde{\boldsymbol{u}}_l, s) + b_l(s, p_l - \tilde{\boldsymbol{p}}_l),$$

which means that $(u_l - \tilde{\boldsymbol{u}}_l, p_l - \tilde{\boldsymbol{p}}_l)$ is a finite element approximation of (z, w) in the space $V_l \times Q_l$. On the other hand, (F_l, s) becomes just the right-hand side of (12) if $s \in V_{l-1}$, i.e., (u_{l-1}^*, p_{l-1}^*) is the finite element approximation of (z, w) in the space $V_{l-1} \times Q_{l-1}$.

Lemma 2.2. *Let $h_{l-1} \leq C h_l$ with a mesh- and level-independent constant C. Then, the approximation property*

$$\|u_l - u_l^{new}\|_H \leq C h_l^2 \|A_l(\underline{u}_l - \underline{\tilde{\boldsymbol{u}}}_l) + B_l^T(\underline{p}_l - \underline{\tilde{\boldsymbol{p}}}_l)\|_{\mathcal{W}_l}$$

holds.

Proof: One can use the same technique which has been presented for the case of a scalar elliptic problem in [4]. □

2.7. Multi-Level Convergence

We shortly describe the two-level algorithm using m smoothing steps on the level l, $l \geq 1$, and the coarse-level correction (12), (13). Let (u_l^0, p_l^0) be an initial guess for the solution (u_l, p_l) of (6), (7). We apply m steps of the basic iteration (11) and obtain (u_l^m, p_l^m). Now, the coarse-level correction (12), (13) is performed using

$$(\tilde{\boldsymbol{u}}_l, \tilde{\boldsymbol{p}}_l) = (u_l^m, p_l^m)$$

as an approximate solution of the discrete problem (6), (7). Finally, the new approximation is obtained by

$$u_l^{new} = u_l^m + \imath_u u_{l-1}^*, \quad p_l^{new} = p_l^m + \imath_p p_{l-1}^*.$$

Combining the smoothing and approximation property, we get

Theorem 2.1. *Under the assumptions of Lemma* 2.1 *and Lemma* 2.2, *the two-level method converges for sufficiently many smoothing steps with respect to the H- and* $\mathscr{U}_l$*-norm. In particular, there are level- and mesh-independent constants C and* $\tilde{C}$ *such that*

$$\|\underline{u}_l - \underline{u}_l^{new}\|_{\mathscr{U}_l} \leq \frac{C}{m} \|\underline{u}_l - \underline{u}_l^0\|_{\mathscr{U}_l}$$

and

$$\|u_l - u_l^{new}\|_H \leq \frac{\tilde{C}}{m} \|u_l - u_l^0\|_H.$$

Proof: Applying Lemma 2.1 we have

$$\|A_l(\underline{u}_l - \underline{u}_l^m) + B_l^T(\underline{p}_l - \underline{p}_l^m)\|_{\mathscr{U}_l} \leq \frac{C}{mh_l^2} \|\underline{u}_l - \underline{u}_l^0\|_{\mathscr{U}_l}.$$

Taking into consideration the norm equivalence (10) and Lemma 2.2, we conclude

$$\begin{aligned} \|\underline{u}_l - \underline{u}_l^{new}\|_{\mathscr{U}_l} &\leq C\|u_l - u_l^{new}\|_H \\ &\leq Ch_l^2 \|A_l(\underline{u}_l - \tilde{\underline{u}}_l) + B_l^T(\underline{p}_l - \tilde{\underline{p}}_l)\|_{\mathscr{U}_l} \\ &\leq \frac{C}{m} \|\underline{u}_l - \underline{u}_l^0\|_{\mathscr{U}_l}, \end{aligned}$$

which proves convergence in the $\mathscr{U}_l$-norm for sufficiently many smoothing steps m. The convergence in the H-norm follows from the norm equivalence (10). □

Remark 2.3. *Note that in our context the notation "two-level" does not necessarily mean that we consider two levels of mesh refinements. Thus, Theorem* 2.1 *is also*

applicable in cases where we have two different finite element discretisations on the same mesh (see Sections 4.2 *and* 4.3*).*

Once proven the convergence of the two-level method, the convergence of the W-cycle multi-level method follows in a standard way (see e.g. [4], [18]). This is also true for a combination of a finite number of different two-level algorithms provided that Theorem 2.1 holds true for each of these two-level methods.

3. A General Transfer Operator

In this section, we will describe general finite element spaces V_l and we will show how then a space Σ_l and a transfer operator $\iota_u : \Sigma_l \to V_l$ satisfying

$$V_{l-1} + V_l \subset \Sigma_l \subset H = L^2(\Omega)^d \tag{14}$$

and the assumptions (H3) and (H4) can be constructed. In this way, the transfer operator can be applied on a large class of finite element spaces. In case of the Stokes problem, for example, also velocity spaces generated by vector-valued basis functions [17] are included.

We denote by $\{\mathscr{T}_l\}_{l\geq 0}$ a family of triangulations of the domain Ω. Each triangulation $\mathscr{T}_l$ consists of a finite number of mutually disjoint simply connected open cells K so that we have

$$\bar{\Omega} = \bigcup_{K\in\mathscr{T}_l} \overline{K}.$$

We assume that

(H6) For any $l > 0$, the triangulation $\mathscr{T}_l$ is obtained from $\mathscr{T}_{l-1}$ by some "refinement", i.e., each cell $K \in \mathscr{T}_{l-1}$ is either a member of $\mathscr{T}_l$ or it has been refined into child cells $K_i \in \mathscr{T}_l$.

In particular, we allow $\mathscr{T}_{l-1} = \mathscr{T}_l$, which gives us the additional possibility to define different finite element spaces V_{l-1} and V_l on the same mesh.

We assume that there exists a finite number of reference domains $\widehat{K}_1, \ldots, \widehat{K}_{\widehat{M}}$ such that, for any level $l \geq 0$ and for any cell $K \in \mathscr{T}_l$, there exists $i \in \{1, \ldots, \widehat{M}\}$ and a one-to-one mapping $F_K \in W^{1,\infty}(\widehat{K}_i, K)$ satisfying

$$F_K(\widehat{K}_i) = K, \quad F_K^{-1} \in W^{1,\infty}(K, \widehat{K}_i). \tag{15}$$

We assume that

$$Ch_K^d \leq |\det \nabla F_K(\hat{x})| \leq \widetilde{C}h_K^d \quad \forall \hat{x} \in \widehat{K}_i, \tag{16}$$

where $h_K = \operatorname{diam}(K)$ and C, $\widetilde{C} > 0$ are independent of K and l. In addition, we suppose that

$$h_K \le C h_{K'} \quad \forall K, K' \in \mathscr{T}_l, \overline{K} \cap \overline{K}' \neq \emptyset \tag{17}$$

and

$$h_K \le C \sup_{B \subset K \text{ is a ball}} \operatorname{diam}(B) \quad \forall K \in \mathscr{T}_l, \tag{18}$$

again with C independent of K, K' and l. The validity of (16)–(18) usually follows from some shape-regularity assumption on the triangulations. Particularly, for simplicial triangulations, the condition (18) already guarantees a shape-regularity of the cells and implies (16). Moreover, if the triangulations satisfy usual compatibility assumptions (cf. e.g. [15]), then (17) also follows. In case of hanging nodes, the difference in the refinement levels of neighbouring elements is limited by (17).

On each reference cell $\widehat{K}_i$, $i = 1, \ldots, \widehat{M}$, we introduce a finite-dimensional space $\widehat{P}_i \subset H^1(\widehat{K}_i)$ having a basis $\{\widehat{\varphi}_{ij}\}_{j=1}^{\dim \widehat{P}_i}$. Employing the mappings F_K from (15), we introduce, for any cell $K \in \mathscr{T}_l$, a finite–dimensional space $\mathbb{P}^l(K) \subset H^1(K)^d$ such that

$$\mathbb{P}^l(K) \subset \{\widehat{v} \circ F_K^{-1} : \widehat{v} \in [\widehat{P}_i]^d\}.$$

We denote by $\varphi_{K,j}$, $j = 1, \ldots, \dim \mathbb{P}^l(K)$, basis functions in $\mathbb{P}^l(K)$ satisfying

$$\varphi_{K,j} = \sum_{k=1}^{\dim \widehat{P}_i} a_{K,jk} (\widehat{\varphi}_{ik} \circ F_K^{-1}), \quad a_{K,jk} \in [-1, 1]^d, \ \ k = 1, \ldots, \dim \widehat{P}_i.$$

Usually, the coefficients $a_{K,jk}$ are zeros or unit vectors in the direction of coordinate axes, and one takes only one non-vanishing coefficient for each j. However, in some cases, also other choices of the coefficients $a_{K,jk}$ may be of use. Particularly, this is the case if the space $\mathbb{P}^l(K)$ contains vector-valued basis functions which cannot be obtained by transforming fixed basis functions from the space $[\widehat{P}_i]^d$ onto K. An example is the Bernardi/Raugel element (cf. [2]) which contains vector-valued basis functions perpendicular to element faces.

We introduce linear functionals $\{\mathscr{N}_{K,i}\}_{i=1}^{\dim \mathbb{P}^l(K)}$ defined on $\mathbb{P}^l(K)$, which we will call local nodal functionals in the following. We assume that these functionals possess the usual duality property with respect to the basis functions, i.e.,

$$\mathscr{N}_{K,i}(\varphi_{K,j}) = \delta_{ij} \qquad \forall i, j = 1, \ldots, \dim \mathbb{P}^l(K),$$

where δ_{ij} denotes the Kronecker symbol. Examples of such nodal functionals can be found in Section 4.

Now, for each level l, we introduce a finite element space V_l satisfying

$$V_l \subset \{w \in L^2(\Omega)^d : w|_K \in \mathbb{P}^l(K) \quad \forall K \in \mathscr{T}_l\}. \tag{19}$$

This space is smaller than the piecewise discontinuous space on the right-hand side of (19) since we assume that there is some connection between functions on neighbouring cells. This connection can be enforced by choosing pairs of nodal functionals from neighbouring cells and by requiring that the two functionals from any pair are equal for any function from the space V_l. We denote by $\{\varphi_{l,i}\}_{i \in I_l}$ a basis of the space V_l obtained in this way, where the set I_l is an index set whose elements will be called nodes in the following. We assume that the mentioned pairs of local nodal functionals were chosen in such a way that, as usual, these basis functions have "small" supports. Precisely, we require that, for any $i \in I_l$, there exists $K \in \mathscr{T}_l$ such that

$$\operatorname{supp}(\varphi_{l,i}) \subset \bigcup_{K' \in \mathscr{T}_l, \overline{K'} \cap \overline{K} \neq \emptyset} \overline{K'}. \tag{20}$$

Further, we assume that, on any cell $K \in \mathscr{T}_l$, the basis functions $\varphi_{l,i}$ coincide with the local basis functions $\varphi_{K,j}$. Thus, denoting by

$$I_l(K) = \{i \in I_l : \operatorname{supp}(\varphi_{l,i}) \cap K \neq \emptyset\}$$

the set of all nodes which are associated with a cell K, it is natural to assume that there exists a one-to-one mapping

$$\pi_K : I_l(K) \to \{1, \ldots, \dim \mathbb{P}^l(K)\}$$

such that

$$\varphi_{l,i}|_K = \varphi_{K,\pi_K(i)} \quad \forall K \in \mathscr{T}_l, \;\; i \in I_l(K).$$

Using the mappings π_K we can renumber the local nodal functionals, i.e., we set

$$N_{K,i} = \mathscr{N}_{K,\pi_K(i)} \quad \forall K \in \mathscr{T}_l, \;\; i \in I_l(K).$$

Then

$$N_{K,i}(\varphi_{l,j}|_K) = \delta_{ij} \quad \forall i, j \in I_l(K).$$

Furthermore, we define for any node $j \in I_l$

$$\mathscr{T}_{l,j} = \{K \in \mathscr{T}_l : j \in I_l(K)\}$$

which is the set of all cells $K \in \mathscr{T}_l$ which are connected with the node j. Then we can give a precise characterisation of the space V_l, namely,

$$V_l = \Big\{ w \in L^2(\Omega)^d : w|_K \in \mathbb{P}^l(K) \quad \forall K \in \mathscr{T}_l, \\ N_{K,i}(w|_K) = N_{K',i}(w|_{K'}) \quad \forall K, K' \in \mathscr{T}_{l,i}, i \in I_l \Big\}.$$

This shows that a natural choice for a global nodal functional is the arithmetic mean of the local nodal functionals

$$N_{l,i}(w) = \frac{1}{\mathrm{card}(\mathscr{T}_{l,i})} \sum_{K \in \mathscr{T}_{l,i}} N_{K,i}(w|_K). \tag{21}$$

Note that we again have the duality relation

$$N_{l,i}(\varphi_{l,j}) = \delta_{ij} \quad \forall\, i,j \in I_l,$$

which implies that

$$w = \sum_{i \in I_l} N_{l,i}(w)\varphi_{l,i} \quad \forall\, w \in V_l. \tag{22}$$

Now, having described the spaces V_l, we can turn to the question how the spaces Σ_l and the mappings $\iota_u : \Sigma_l \to V_l$ satisfying (14), (H3) and (H4) can be defined. Following the ideas developed in [31], where the construction of general transfer operators for finite element spaces has been investigated, we construct Σ_l as a discontinuous finite element space

$$\Sigma_l = \left\{ w \in L^2(\Omega)^d : w|_K \in \mathbb{S}^l(K) \quad \forall K \in \mathscr{T}_l \right\}$$

with a finite dimension. To guarantee (14), we furthermore assume that

(H7) The local function space $\mathbb{S}^l(K)$ is constructed such that

$$\mathbb{P}^{l-1}(\mathscr{F}(K))|_K + \mathbb{P}^l(K) \subset \mathbb{S}^l(K) \quad \forall K \in \mathscr{T}_l$$

where $\mathscr{F}(K) \in \mathscr{T}_{l-1}$ is the parent cell of a child cell $K \in \mathscr{T}_l$ for $K \in \mathscr{T}_l \setminus \mathscr{T}_{l-1}$ and $\mathscr{F}(K) = K$ for $K \in \mathscr{T}_l \cap \mathscr{T}_{l-1}$.

We suppose that, for any $K \in \mathscr{T}_l$, the local nodal functionals $N_{K,i}$ are well defined on $\mathbb{S}^l(K)$, which usually means that the functions in $\mathbb{S}^l(K)$ are of the same type as those in $\mathbb{P}^l(K)$ (e.g., continuous). Then we can define the transfer operator $\iota_u : \Sigma_l \to V_l$ simply by

$$\iota_u w = \sum_{i \in I_l} N_{l,i}(w)\varphi_{l,i}, \quad w \in \Sigma_l. \tag{23}$$

In view of (22) we immediately obtain the validity of (H3). To be able to prove (H4), we assume that each of the spaces $\mathbb{S}^l(K)$ can be obtained by transforming functions from one of the reference cells onto K. Thus, we introduce finite element spaces $\widehat{S}_i \subset H^1(\widehat{K}_i)^d$, $i = 1, \ldots, \widehat{M}$, with bases $\{\widehat{\psi}_{ij}\}_{j=1}^{\dim \widehat{S}_i}$ and we assume that, for any $K \in \mathscr{T}_l$, there exists $i \in \{1, \ldots, \widehat{M}\}$ such that

$$\mathbb{S}^l(K) = \{\widehat{v} \circ F_K^{-1} : \widehat{v} \in \widehat{S}_i\}, \tag{24}$$

$$\left|N_{K,m}(\widehat{\psi}_{ij} \circ F_K^{-1})\right| \leq C \quad \forall\, m \in I_l(K),\ \ j \in \{1, \ldots, \dim \widehat{S}_i\}, \tag{25}$$

where F_K is the mapping from (15) and C is independent of K and l. The last assumption is automatically satisfied if the local nodal functionals $N_{K,i}$ are defined by means of a finite number of functionals defined on the reference spaces $\widehat{S}_i$, which is often the case.

Lemma 3.1. *The operator ι_u defined by* (23) *is uniformly L^2-stable, i.e., it satisfies* (H4) *with a constant C independent of l and with $\|\cdot\|_H = \|\cdot\|_0 \equiv \|\cdot\|_{L^2(\Omega)}$.*

Proof: Consider any $w \in \Sigma_l$ and any $K \in \mathscr{T}_l$ and let F_K and $\widehat{S}_i$ be the mapping and the space from (24), respectively. Then

$$w|_K = \sum_{j=1}^{\dim \hat{S}_i} w_j (\widehat{\psi}_{ij} \circ F_K^{-1})$$

for some real numbers w_j and it follows from (25), from the equivalence of norms on finite-dimensional spaces and from (16) that, for any $m \in I_l(K)$,

$$|N_{K,m}(w|_K)| \leq C \sum_{j=1}^{\dim \hat{S}_i} |w_j| \leq \widetilde{C} \|w \circ F_K\|_{0,\widehat{K}_i} \leq \bar{C} h_K^{-d/2} \|w\|_{0,K}.$$

Thus, we see that, for any $i \in I_l$, we have

$$|N_{l,i}(w)| \leq C \sum_{K \in \mathscr{T}_{l,i}} h_K^{-d/2} \|w\|_{0,K}. \tag{26}$$

For any cell $\widetilde{K} \in \mathscr{T}_l$, we derive using (16), (26), (20) and (17) that

$$\|\iota_u w\|_{0,\widetilde{K}} = \left\| \sum_{i \in I_l(\widetilde{K})} N_{l,i}(w) \varphi_{l,i} \right\|_{0,\widetilde{K}} \leq C h_{\widetilde{K}}^{d/2} \sum_{i \in I_l(\widetilde{K})} |N_{l,i}(w)| \leq \widetilde{C} \sum_{K \subset \delta(\widetilde{K})} \|w\|_{0,K},$$

where we denoted by

$$\delta(\widetilde{K}) = \bigcup_{i \in I_l(\widetilde{K})} \bigcup_{K \in \mathscr{T}_{l,i}} K$$

the vicinity of any cell $\widetilde{K} \in \mathscr{T}_l$. In view of (17), (18) and (20), the number of cells in $\delta(\widetilde{K})$ is bounded independently of $\widetilde{K}$ and l and hence we obtain

$$\|\iota_u w\|_{0,K} \leq C \|w\|_{0,\delta(K)} \quad \forall\, w \in \Sigma_l,\ \ K \in \mathscr{T}_l,$$

which expresses a local L^2-stability of the operator ι_u. Again, according to (17), (18) and (20), the number of the sets $\delta(\widetilde{K})$ which contain any fixed cell $K \in \mathscr{T}_l$ is bounded independently of l and hence the local L^2-stability of ι_u immediately implies the global L^2-stability (H4). □

A significant step in the above considerations was the assumption that there exist spaces $\mathbb{S}^l(K)$ satisfying (H7) and (24). In the remaining part of this section, we will prove that this is true for simplicial finite elements. Thus, from now on, we assume that there is only one reference cell $\widehat{K}$, which is a d-simplex. It is essential for our further proceeding that, for any simplicial cell K, there exists a regular affine mapping $F_K : \widehat{K} \to K$ which maps $\widehat{K}$ onto K. We denote the set of all these mappings by $\mathscr{L}_R(\widehat{K}, K)$.

Like above, we introduce a fixed finite-dimensional space $\widehat{P} \subset H^1(\widehat{K})^d$ and we assume that, for any $K \in \mathscr{T}_l$ and any $F_K \in \mathscr{L}_R(\widehat{K}, K)$, we have

$$\mathbb{P}^l(K) \subset \{\widehat{v} \circ F_K^{-1} : \widehat{v} \in \widehat{P}\}.$$

We assume that, as usual, the cells of the triangulations are refined according to a finite number of geometrical rules. Therefore, the refinements of all cells K can be mapped by the linear mappings F_K^{-1} onto a finite number $\widehat{L}$ of refinements of the reference cell $\widehat{K}$ into child cells $\widehat{K}_{i,1}, \ldots, \widehat{K}_{i,\widehat{M}_i}$, $i = 1, \ldots, \widehat{L}$. That means that, for any cell $K \in \mathscr{T}_l$ obtained by refining a parent cell $\mathscr{F}(K) \in \mathscr{T}_{l-1}$ and for any $F_{\mathscr{F}(K)} \in \mathscr{L}_R(\widehat{K}, \mathscr{F}(K))$, there exist indices $i \in \{1, \ldots, \widehat{L}\}$ and $j \in \{1, \ldots, \widehat{M}_i\}$ such that $K = F_{\mathscr{F}(K)}(\widehat{K}_{ij})$. We denote

$$\widehat{P}_{ij} = \{\widehat{v} \circ F_{\widehat{K}_{ij}} : \widehat{v} \in \widehat{P}, F_{\widehat{K}_{ij}} \in \mathscr{L}_R(\widehat{K}, \widehat{K}_{ij})\}.$$

Then, for any $v \in \mathbb{P}^{l-1}(\mathscr{F}(K))$ and any $F_K \in \mathscr{L}_R(\widehat{K}, K)$, there exists $\widehat{w} \in \widehat{P}_{ij}$ such that

$$v|_K = \widehat{w} \circ F_K^{-1}.$$

Indeed, $v = \widehat{v} \circ F_{\mathscr{F}(K)}^{-1}$ for some $\widehat{v} \in \widehat{P}$ and hence

$$v|_K = \widehat{v} \circ (F_{\mathscr{F}(K)}^{-1} \circ F_K) \circ F_K^{-1},$$

where $F_{\mathscr{F}(K)}^{-1} \circ F_K \in \mathscr{L}_R(\widehat{K}, \widehat{K}_{ij})$. Thus, for any $K \in \mathscr{T}_l$ and any $F_K \in \mathscr{L}_R(\widehat{K}, K)$, we have

$$\mathbb{P}^{l-1}(\mathscr{F}(K))|_K \subset \{\widehat{v} \circ F_K^{-1} : \widehat{v} \in \widehat{P}_{ij}\}$$

for some indices $i \in \{1, \ldots, \widehat{L}\}$ and $j \in \{1, \ldots, \widehat{M}_i\}$. Now, we define

$$\widehat{S} = \operatorname{span}\left\{ \widehat{P} \cup \bigcup_{i=1}^{\widehat{L}} \bigcup_{j=1}^{\widehat{M}_i} \widehat{P}_{ij} \right\}$$

and, for any $K \in \mathscr{T}_l$, we choose some $F_K \in \mathscr{L}_R(\widehat{K}, K)$ and set

$$\mathbb{S}^l(K) = \{\widehat{v} \circ F_K^{-1} : \widehat{v} \in \widehat{S}\}.$$

It is easy to see that these spaces $\mathbb{S}^l(K)$ satisfy the assumption (H7).

4. Applications to the Stokes Equations

In this section we give details how the general assumptions made in Section 3 can be fulfilled for the Stokes problem. In particular, we will show that the usually used multi-grid technique for the nonconforming finite elements of lowest order coincides with the use of the general transfer operator described in the preceding section.

4.1. Lowest Order Nonconforming Elements

Our first examples are the nonconforming finite elements of first order on triangles and quadrilaterals. The triangular element was introduced by Crouzeix and Raviart and analysed in [16]. The element on quadrilaterals was established by Rannacher and Turek and analysed in [26, 30].

We consider a hierarchy of uniformly refined grids. Let $\mathscr{T}_0$ be a regular triangulation of $\Omega \subset \mathbb{R}^2$ into triangles or into convex quadrilaterals. The mesh $\mathscr{T}_l$ is obtained from $\mathscr{T}_{l-1}$ by subdividing each cell of $\mathscr{T}_{l-1}$ into four child cells. For triangles, we connect the midpoints of the edges. In the quadrilateral case, we connect the midpoints of opposite edges.

Now we construct the finite element spaces V_l. Let $P_1(K)$ be the space of linear polynomials on the triangle K. The space of rotated bilinear functions on a quadrilateral K is defined by

$$Q_1^{rot}(K) = \{\hat{q} \circ F_K^{-1} : \hat{q} \in \text{span}(1, \hat{x}, \hat{y}, \hat{x}^2 - \hat{y}^2)\}$$

where $F_K : \hat{K} \to K$ is the bilinear reference transformation from the reference cell $\hat{K} = (-1, 1)^2$ onto the cell K, see [26, 30]. Let $\mathscr{E}(K)$ denote the set of all edges of the element K. We define for any $E \in \mathscr{E}(K)$ the nodal functional

$$N_E^K(v) = \frac{1}{|E|} \int_E v|_K \, ds.$$

Let $\mathscr{E}^l = \bigcup_{K \in \mathscr{T}_l} \mathscr{E}(K)$ be the set of all edges of $\mathscr{T}_l$. The set $\mathscr{E}^l_{\partial\Omega} = \{E \in \mathscr{E}^l : E \subset \partial\Omega\}$ contains all boundary edges. The finite element space V_l is given by

$$V_l = \{v \in L^2(\Omega)^2 : v|_K \in P(K)^2 \ \forall K \in \mathscr{T}_l,$$
$$N_E^K(v) = N_E^{K'}(v) \ \forall E \in \mathscr{E}(K) \cap \mathscr{E}(K'), K, K' \in \mathscr{T}_l, \quad N_E^K(v) = 0 \ \forall E \in \mathscr{E}^l_{\partial\Omega}\}$$

where $P(K)$ is $P_1(K)$ on triangles and $Q_1^{rot}(K)$ on quadrilaterals.

Since the triangulation $\mathscr{T}_l$ is obtained from $\mathscr{T}_{l-1}$ by regular refinement of all cells, we have $\mathscr{T}_l \cap \mathscr{T}_{l-1} = \emptyset$. Let us show that the assumptions (H7) and (24) hold. In the case of triangles, the inclusion $\mathbb{P}^{l-1}(\mathscr{F}(K))|_K \subset P_1(K)^2$ follows directly from the affine reference mapping and we have $\mathbb{P}^{l-1}(\mathscr{F}(K))|_K + \mathbb{P}^l(K) \subset P_1(K)^2$. Thus, we can choose $\mathbb{S}^l(K) = P_1(K)^2$. The situation is more complicated for the Q_1^{rot} element. Let us consider $K \in \mathscr{T}_{l-1}$ and let $K_1, \ldots, K_4 \in \mathscr{T}_l$ be the child cells of K. We set $\hat{K}_i = F_K^{-1}(K_i)$, $i = 1, \ldots, 4$ (cf. Fig. 1). Let for example $q \in \mathbb{P}^{l-1}(\mathscr{F}(K_1))|_{K_1}$ which means that there is a function

$$\hat{q} \in \operatorname{span}(1, \hat{x}_1, \hat{x}_2, \hat{x}_1^2 - \hat{x}_2^2) \quad \text{with } q = (\hat{q} \circ F_K^{-1})\big|_{K_1}.$$

The mapping $G_1 : \hat{K} \to \hat{K}_1$ given by

$$\hat{x}_1 \mapsto (1 + \hat{x}_1)/2, \quad \hat{x}_2 \mapsto (1 + \hat{x}_2)/2$$

and $F_K\big|_{\hat{K}_1} : \hat{K}_1 \to K_1$ are bijective. Thus, we have $F_{K_1} = F_K\big|_{\hat{K}_1} \circ G_1$ and get

$$q \circ F_{K_1} = \hat{q} \circ F_K^{-1}|_{K_1} \circ F_{K_1} = \hat{q} \circ F_K^{-1}|_{K_1} \circ F_K\big|_{\hat{K}_1} \circ G_1 = \hat{q} \circ G_1.$$

Since the local space $\operatorname{span}(1, \hat{x}_1, \hat{x}_2, \hat{x}_1^2 - \hat{x}_2^2)$ is invariant with respect to the mapping G_1 we conclude $\mathbb{P}^{l-1}(\mathscr{F}(K_1))|_{K_1} \subset \mathbb{P}^l(K_1)$. The same arguments can be applied to K_i, $i = 2, 3, 4$, which results in

$$\mathbb{P}^{l-1}(\mathscr{F}(K))|_K + \mathbb{P}^l(K) \subset Q_1^{rot}(K)^2 \quad \text{for all quadrilaterals } K \in \mathscr{T}_l.$$

This allows us to choose $\mathbb{S}^l(K) = Q_1^{rot}(K)^2$ in the definition of the space Σ_l. Note that the assumptions (24) and (25) are then fulfilled.

The finite element spaces V_{l-1} and V_l are non-nested. In order to get a suitable prolongation we will use the general transfer operator which was introduced in

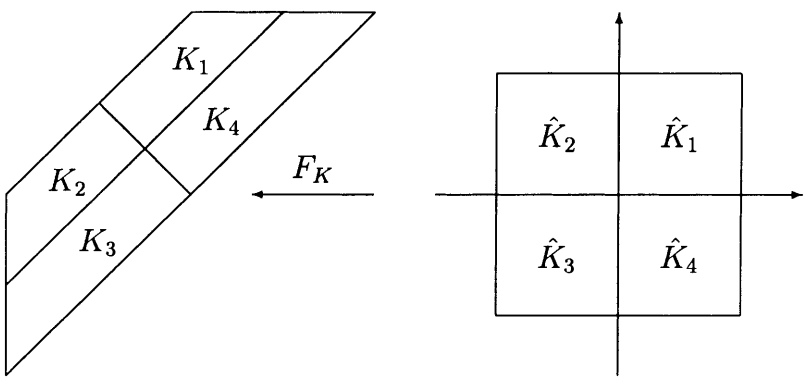

Figure 1. Refinement of original and reference cell

Section 3. The definition of the global nodal functionals (21) simplifies for the above spaces to

$$N_E(w) = \frac{1}{2}\left(N_E^K(w) + N_E^{K'}(w)\right)$$

for all inner edges E with the neighbouring elements K and K'. For boundary edges we get

$$N_E(w) = N_E^K(w)$$

where $E \in \mathscr{E}(K)$. The resulting mapping $\imath_u$ is the same as in [21].

The space Q_l which approximates the pressure consists of piecewise constant functions, i.e.,

$$Q_l = \{q \in L_0^2(\Omega) : q|_K \in P_0(K) \ \ \forall K \in \mathscr{T}_l\}.$$

For the proof of assumption (H2) we refer to [16, 26]. Since $Q_{l-1} \subset Q_l$ the transfer operator $\imath_p$ is the identity.

For numerical experiments with the Crouzeix–Raviart element we refer to [21].

4.2. Modified Crouzeix–Raviart Element

It is sometimes necessary to use other types of boundary conditions than the Dirichlet boundary condition considered in (3). For example, if a part Γ_N of $\partial\Omega$ represents a free surface of a fluid, then one can use the boundary conditions

$$(I - n \otimes n)[\nabla u + (\nabla u)^T] = 0, \quad u \cdot n = 0 \quad \text{on } \Gamma_N, \tag{27}$$

where I is the identity tensor and n is the outer normal vector to Γ_N. The first condition in (27) states that zero surface forces act in the tangential direction to Γ_N. The boundary conditions (27) generally do not allow to use the bilinear form a defined in (4) and instead we have to consider

$$a(u, v) = \frac{1}{2}\int_\Omega \left(\nabla u + (\nabla u)^T\right) : \left(\nabla v + (\nabla v)^T\right) dx.$$

If $\text{meas}_{d-1}(\partial\Omega \setminus \Gamma_N) > 0$, then the ellipticity of this bilinear form for functions from $H^1(\Omega)^d$ vanishing on $\partial\Omega \setminus \Gamma_N$ is assured by the Korn inequality. However, the *discrete* Korn inequality does not hold for most first order nonconforming finite element spaces (cf. [23]), particularly, it fails for the elements investigated in the preceding section. Consequently, in these cases, the validity of (H2) cannot be shown.

One of the few first order nonconforming elements which do not violate the discrete Korn inequality is the modified Crouzeix–Raviart element P_1^{mod} which was developed in [25] for solving convection dominated problems. Here we confine ourselves to a particular example of this element for which the space of shape functions on the reference triangle $\widehat{K}$ is

$$\widehat{P} = \mathrm{span}\{\widehat{\lambda}_1, \widehat{\lambda}_2, \widehat{\lambda}_3, \widehat{\lambda}_1^2\widehat{\lambda}_2 - \widehat{\lambda}_2^2\widehat{\lambda}_1, \widehat{\lambda}_2^2\widehat{\lambda}_3 - \widehat{\lambda}_3^2\widehat{\lambda}_2, \widehat{\lambda}_3^2\widehat{\lambda}_1 - \widehat{\lambda}_1^2\widehat{\lambda}_3\},$$

where $\widehat{\lambda}_1$, $\widehat{\lambda}_2$, $\widehat{\lambda}_3$ are the barycentric coordinates on $\widehat{K}$. To each edge $\widehat{E}$ of $\widehat{K}$, we assign two nodal functionals, $\widehat{N}_{\widehat{E},1}$ and $\widehat{N}_{\widehat{E},2}$, defined by

$$\widehat{N}_{\widehat{E},1}(\widehat{v}) = \frac{1}{|\widehat{E}|}\int_{\widehat{E}} \widehat{v}\, d\widehat{s}, \quad \widehat{N}_{\widehat{E},2}(\widehat{v}) = \frac{60}{|\widehat{E}|}\int_{\widehat{E}} \widehat{v}\left(\widehat{\lambda}_{\widehat{E}} - \frac{1}{2}\right) d\widehat{s},$$

where $\widehat{\lambda}_{\widehat{E}}$ is a barycentric coordinate on $\widehat{E}$. The space V_l is now obtained by transforming the space $\widehat{P}$ and the six nodal functionals $\widehat{N}_{\widehat{E},1}$, $\widehat{N}_{\widehat{E},2}$, $\widehat{E} \subset \partial\widehat{K}$, onto the cells of the triangulation by means of regular affine mappings (cf. the preceding section). In this way, we get the space

$$V_l = \Big\{ v \in L^2(\Omega)^2 : v|_K \in P(K)^2 \ \ \forall K \in \mathscr{T}_l, . \\ \int_E [|v|]_E q\, ds = 0 \ \ \forall q \in P_1(E), \ \ E \in \mathscr{E}^l \Big\},$$

where $[|v|]_E$ denotes the jump of v across the edge E,

$$P(K) = \mathrm{span}\{\lambda_1, \lambda_2, \lambda_3, \lambda_1^2\lambda_2 - \lambda_2^2\lambda_1, \lambda_2^2\lambda_3 - \lambda_3^2\lambda_2, \lambda_3^2\lambda_1 - \lambda_1^2\lambda_3\}$$

and λ_1, λ_2, λ_3 are the barycentric coordinates on the cell K. A nice property of the P_1^{mod} element is that

$$\int_E [|v|]_E q\, ds = 0 \quad \forall v \in V_l, \ \ q \in P_2(E), \ \ E \in \mathscr{E}^l.$$

It is easy to verify that the assumptions made in Section 3 are satisfied. The assumption (H2) holds if the space Q_l consists of discontinuous piecewise linear functions from $L_0^2(\Omega)$ and each cell has at least one vertex in Ω since then an inf-sup condition holds (cf. [24] and [16]). Consequently, (H2) is also satisfied if Q_l is a subspace of $L_0^2(\Omega)$ consisting e.g. of piecewise constant functions, continuous piecewise linear functions or nonconforming piecewise linear functions.

Here we present numerical results for Q_l consisting of piecewise constant functions so that the transfer operator ι_p can be replaced by the identity. The discretisations are defined on a sequence of uniformly refined triangular grids starting with the triangular grid from Fig. 2 which we denote as $\mathscr{T}_0$ (level 0). We shall consider two kinds of multi-level solvers for solving the Stokes equations on a given geometrical mesh level. The first one is a classical multi-level method

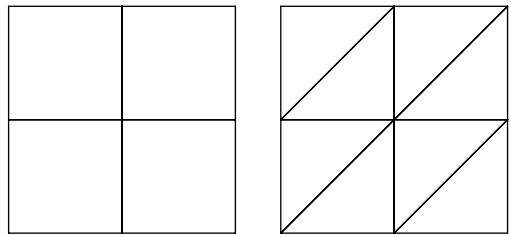

Figure 2. Coarsest grids (level 0)

where each mesh corresponds to one level of the algorithm and on each mesh we consider a discrete problem of the same type, i.e., the Stokes equations discretised using the P_1^{mod}/P_0 element. In the second multi-level solver, the discretisation using the P_1^{mod}/P_0 element is used on the finest mesh $\mathscr{T}_L$ only and on all other mesh levels a 'cheaper' discretisation is employed, namely the Crouzeix–Raviart element with piecewise constant pressure denoted as P_1^{nc}/P_0. In addition, the P_1^{nc}/P_0 discretisation is also applied on the finest mesh level $\mathscr{T}_L$ so that two different discretisations corresponding to two levels of the multi-level method are considered on the finest geometrical mesh. We refer to the next section for more details on this multiple discretisation multi-level approach. Note that both kinds of multi-level solvers fit into the framework of this paper and the prolongations and restrictions can be defined using the general transfer operator $\imath_u$ described above. The numbers of degrees of freedom to which the mentioned discretisations lead on different meshes are given in Table 3.

As a smoother, we use the basic iteration described in Section 2.5. Therefore, the system (11) has to be solved in each smoothing step which implies that the efficient solution of (11) is essential for the efficiency of the multi-level solver. In view of an application of our procedure to the Navier–Stokes equations [19], where A_l and D_l are no longer symmetric, we solve (11) iteratively by a preconditioned flexible GMRES method, see e.g. [27]. The preconditioner is defined via the pressure Schur complement equation of (11)

$$B_l(\alpha_l D_l)^{-1} B_l^T (\underline{p}_l^{j+1} - \underline{p}_l^j) = B_l(\alpha_l D_l)^{-1} \underline{r}_l^j - \underline{s}_l^j, \tag{28}$$

where

$$\begin{pmatrix} \underline{r}_l^j \\ \underline{s}_l^j \end{pmatrix} = \begin{pmatrix} \underline{f}_l \\ 0 \end{pmatrix} - \begin{pmatrix} A_l & B_l^T \\ B_l & 0 \end{pmatrix} \begin{pmatrix} \underline{u}_l^j \\ \underline{p}_l^j \end{pmatrix}$$

is the right-hand side of (11). First, (28) is solved approximately by some steps of the standard GMRES method by Saad and Schultz [28] providing the approximation $\tilde{\underline{p}}_l$ of $\underline{p}_l^{j+1} - \underline{p}_l^j$. Second, an approximation $\tilde{\underline{u}}_l$ of $\underline{u}_l^{j+1} - \underline{u}_l^j$ is computed by

$$\tilde{\underline{u}}_l = (\alpha_l D_l)^{-1} (\underline{r}_l^j - B_l^T \tilde{\underline{p}}_l).$$

The solution of (11) is the most time consuming part of the multi-grid iteration. It was shown by Zulehner [36] that the smoothing property of the Braess–Sarazin smoother is maintained if (11) is solved only approximately as long as the approximation is close enough to the solution. Numerical experiments show that, in general, one obtains similar rates of convergence of the multi-level algorithm like with an exact solution of (11). Considering the efficiency of the multi-level solver measured in computing time, the variant with the approximate solution is in general considerably better and therefore it is used in practice. Thus, in the computations presented below we stopped the solution of (11) after the Euclidean norm of the residual has been reduced by the factor 10. The systems on level 0 were solved exactly.

We shall present numerical results for the following

Example 4.1. *W-cycle in a 2d test case*. We consider the Stokes problem in $\Omega = (0,1)^2$ with the prescribed solution

$$\begin{aligned} u(x,y) &= (\sin x \sin y, \cos x \cos y)^T, \\ p(x,y) &= 2\cos x \sin y - 2\sin 1(1-\cos 1), \\ f(x,y) &= (0, 4\cos x \cos y)^T. \end{aligned}$$

This example is taken from the paper [5] by Braess and Sarazin.

The computations were performed using the $W(m,m)$-cycle, $D_l = SSOR(A_l)$ and $\alpha_l = 1.0$. Table 1 shows the geometric means of the error reduction rates

$$\frac{\|u_l - u_l^{new}\|_0}{\|u_l - u_l^0\|_0}$$

for the multi-level solver which uses the P_1^{mod}/P_0 discretisations on all levels. Table 2 shows the averaged error reduction rates for the multi-level solver which combines the use of the P_1^{mod}/P_0 discretisation on the finest level with the use of P_1^{nc}/P_0 discretisations on all lower levels. We observe that, for each m, the error reduction rates can be bounded by a level-independent constant as predicted by Theorem 2.1. In addition, it can be clearly seen from the two tables that, for

Table 1. Example 4.1, P_1^{mod}/P_0, $D_l = SSOR(A_l)$, $\alpha_l = 1.0$, $W(m,m)$-cycle, averaged error reduction rates

m	mesh level				
	1	2	3	4	5
1	6.29e-1	6.75e-1	6.95e-1	7.12e-1	7.11e-1
2	4.73e-1	5.25e-1	5.56e-1	5.62e-1	5.60e-1
3	3.65e-1	4.26e-1	4.55e-1	4.60e-1	4.56e-1
4	2.83e-1	3.48e-1	3.78e-1	3.81e-1	3.74e-1
5	2.20e-1	2.87e-1	3.13e-1	3.13e-1	3.08e-1
6	1.70e-1	2.36e-1	2.62e-1	2.62e-1	2.59e-1

Table 2. Example 4.1, P_1^{mod}/P_0 on finest level combined with P_1^{nc}/P_0 on lower levels, $D_l = SSOR(A_l)$, $\alpha_l = 1.0$, $W(m,m)$-cycle, averaged error reduction rates

m	mesh level				
	1	2	3	4	5
1	9.44e-1	9.98e-1	1.04e-0	1.02e-0	1.01e-0
2	3.84e-1	4.34e-1	4.31e-1	4.26e-1	4.14e-1
3	1.89e-1	2.51e-1	2.48e-1	2.42e-1	2.41e-1
4	1.17e-1	1.87e-1	1.78e-1	1.75e-1	1.77e-1
5	8.35e-2	1.50e-1	1.33e-1	1.31e-1	1.30e-1
6	6.17e-2	1.27e-1	1.06e-1	1.01e-1	1.02e-1

$m > 1$, the multi-level method which uses the Crouzeix–Raviart element on lower levels converges faster than the standard multi-level method.

4.3. A Multi-Grid Method for Higher Order Discretisations Based on Lowest Order Nonconforming Discretisations

As the last and certainly most important application, we consider a multi-grid method for higher order discretisations which is based on lowest order nonconforming discretisations on the coarser multi-grid levels. Like in the previous section, we use a multiple discretisation multi-level approach with two different discretisations on the finest geometric mesh level L, i.e., the spaces for the multi-grid levels L and $L+1$ are defined both on $\mathscr{T}_L$, see Fig. 3. The higher order discretisation is used on multi-grid level $L+1$ whereas on all coarser levels l, $0 \leq l \leq L$, a nonconforming discretisation of lowest order is applied.

Remark 4.1. *The construction of this multiple discretisation multi-level approach was inspired by numerical studies of benchmark problems for the steady state Navier–Stokes equations in* [19, 20]. *These studies show on the one hand a dramatic improvement of benchmark reference values using higher order discretisations in comparison to lowest order nonconforming discretisations. On the other hand, the arising systems of equations for the lowest order nonconforming discretisations could be solved very fast and efficiently with the standard multi-grid approach. This standard multi-grid approach showed a very unsatisfactory behaviour for all higher order discretisations. Often, it did not converge at all. Sometimes, convergence could be achieved by heavily damping, leading to a bad rate of convergence and a very inefficient solver. These difficulties could be overcome by applying the multi-grid method described in this section. Thus, this method has been proved already to be a powerful tool in the numerical solution of Navier–Stokes equations combining the superior accuracy of higher order discretisations and the efficiency of multi-grid solvers for lowest order nonconforming discretisations.*

In case of the Stokes problem, the proposed multi-grid method fits into the framework of this paper. Between the lower levels l and $l+1$ of the multi-grid hierarchy, $0 \leq l < L$, we use the transfer operators which have been defined in Section 4.1. To define the transfer operator between the levels L and $L+1$, both

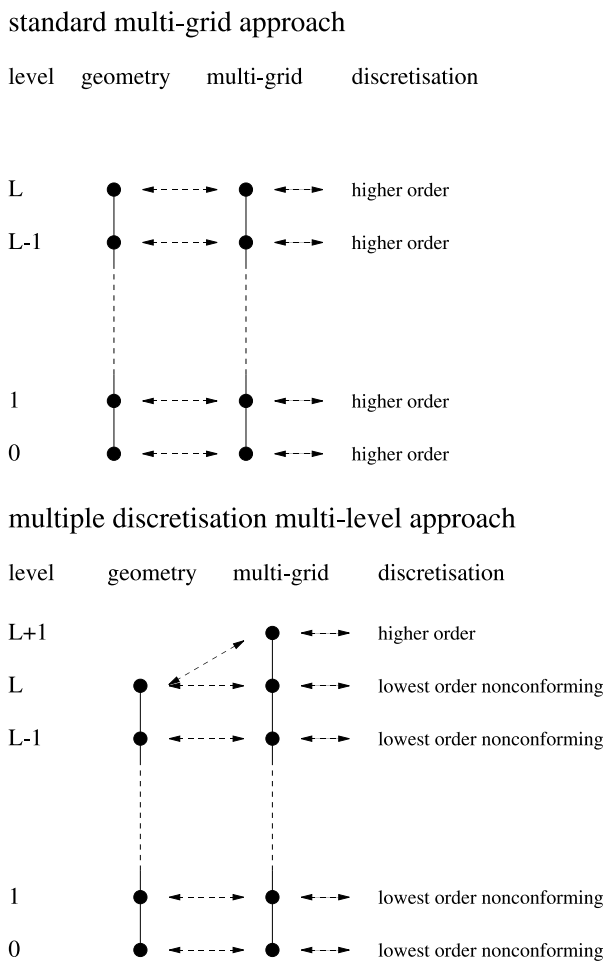

Figure 3. A comparison between the standard and the multiple discretisation multi-level approach

mappings $\imath_u$ and $\imath_p$ have to be constructed since in general $V_L \not\subset V_{L+1}$ and for some higher order discretisations also $Q_L \not\subset Q_{L+1}$. The construction can be done by applying the techniques from Section 3. We choose

$$\Sigma_{L+1} = \left\{ v \in L^2(\Omega) : v|_K \in \mathbb{P}^{L+1}(K) \;\; \forall K \in \mathscr{T}_L = \mathscr{T}_{L+1} \right\},$$

where $\mathbb{P}^{L+1}(K)$ is the space of local shape functions of the corresponding finite element spaces V_{L+1} and Q_{L+1}, respectively.

We will present numerical results obtained with this multi-grid technique for a number of higher order finite element discretisations. Let P_0 and Q_0 denote the spaces of piecewise constant functions on simplicial mesh cells and quadrilateral/hexahedral mesh cells, respectively. By $P_k, Q_k, k \geq 1$, we denote the well-known finite element spaces of continuous functions of piecewise k-th degree. The

notation P_k^{disc} is used for spaces of discontinuous functions whose restriction to each mesh cell is a polynomial of degree k. The Crouzeix–Raviart finite element space is again denoted by P_1^{nc}.

Three examples for the multi-level approach for higher order discretisations will be considered. The first example confirms the theoretical results of Theorem 2.1, i.e., we consider a two-level method and solve the systems (11) arising in the smoothing process exactly. The solution procedure was described in the preceding section. Then we consider Example 4.1 from the previous section and Example 4.4 defined below to demonstrate the behaviour of the multi-level W-cycle with approximated solutions of (11) for test problems in 2d and 3d.

Example 4.2. *Two-level method.* This example has been designed to check the theoretically predicted results with respect to the two-level method. We consider the Stokes equations (3) in $\Omega = (0,1)^2$ with $f = 0$, such that $u = 0$, $p = 0$ is the solution of (3). The computations were carried out on a sequence of meshes starting with level 0 (see Fig. 2), for which the corresponding numbers of the degrees of freedom are given in Table 3. The discrete solution on each level is $u_l = 0$, $p_l = 0$. Since we consider a two-level method, there is only one mesh level in a specific computation. On this geometric mesh level, the lowest order nonconforming discretisation of (3) defines the coarse level in the two-level method and a higher order discretisation the fine level.

As initial guess of the two-level method for each computation, we have chosen $u_{l,i} = 1$ for all interior degrees of freedom and $p_{l,i} = 0$. Thus, the initial error is smooth. The results presented in Table 4 were obtained with 3 pre-smoothing steps, without post-smoothing, and with $\alpha_l D_l = 1.5\mathrm{diag}(A_l)$. Thus, we have exactly the situation investigated in Section 2.

The results of the numerical studies are given in Table 4 and Fig. 4. Table 4 shows the averaged error reduction rate for the two-level method applied to a number of higher order discretisations. It can be clearly seen that the error reduction rate is

Table 3. Degrees of freedom for the discretisations in the 2d test cases, Example 4.1 and 4.2

disc.	mesh level							
	1	2	3	4	5	6	7	8
Q_1^{rot}/Q_0	96	352	1344	5248	20736	82432	328704	1312768
P_1^{nc}/P_0	144	544	2112	8320	33024	131584	525312	2099200
P_1^{mod}/P_0	256	960	3712	14592	57856	230400	919552	3674112
Q_2/Q_1	187	659	2467	9539	37507	148739	592387	2364419
Q_2/P_1^{disc}	210	770	2946	11522	45570	181250	722946	2887682
P_2/P_1	187	659	2467	9539	37507	148739	592387	2364419
Q_3/Q_2	419	1539	5891	23043	91139	362499	1445891	
Q_3/P_2^{disc}	434	1634	6338	24962	99074	394754	1575938	
P_3/P_2	419	1539	5891	23043	91139	362499	1445891	
Q_4/Q_3	747	2803	10851	42691	169347	674563		
Q_4/P_3^{disc}	738	2818	11010	43522	173058	690178		

Table 4. Example 4.2, $D_l = \mathrm{diag}(A_l)$, $\alpha_l = 1.5$, 3 pre-smoothing steps, no post-smoothing, averaged error reduction rates

disc.	mesh level					
	1	2	3	4	5	6
Q_2/Q_1	8.51e-2	1.31e-1	1.34e-1	1.29e-1	1.30e-1	1.27e-1
Q_2/P_1^{disc}	2.80e-2	6.01e-2	6.64e-2	6.68e-2	6.61e-2	6.70e-2
P_2/P_1	2.19e-1	2.72e-1	2.81e-1	2.79e-1	2.76e-1	2.72e-1
Q_3/Q_2	2.84e-1	3.37e-1	3.50e-1	3.53e-1	3.54e-1	
Q_3/P_2^{disc}	2.84e-1	2.93e-1	3.08e-1	3.09e-1	3.10e-1	
P_3/P_2	7.32e-1	8.45e-1	8.46e-1	8.38e-1	8.34e-1	
Q_4/P_3^{disc}	6.71e-1	6.72e-1	6.62e-1	6.55e-1		

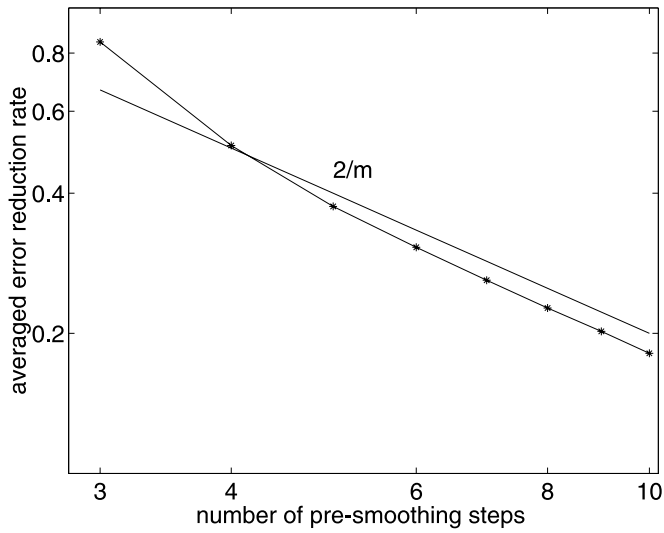

Figure 4. Example 4.2, averaged error reduction rate for different numbers of pre-smoothing steps, P_3/P_2 discretisation, mesh level 4

for all discretisations independent of the level as stated in Theorem 2.1. The second statement of Theorem 2.1, the decrease of the error reduction rate by $\mathcal{O}(1/m)$, where m is the number of pre-smoothing steps, is illustrated for the P_3/P_2 discretisation on mesh level 4 in Fig. 4. The situation is quite similar for the other higher order discretisations.

Example 4.3. *Example 4.1 continued.* Now let us turn back to Example 4.1 formulated in the preceding section. Table 5 shows the averaged error reduction rates obtained for higher order discretisations with the $W(1,1)$-cycle, $D_l = ILU(A_l)$ and $\alpha_l = 1.0$. When solving (11) by the flexible GMRES method the reduction of the Euclidean norm of the residual by the factor 10 was often achieved with the first flexible GMRES steps. We applied 10 iteration steps each time in the GMRES method for solving the pressure Schur complement equation (28).

Table 5. Example 4.3, $D_l = ILU(A_l)$, $\alpha_l = 1.0$, $W(1,1)$-cycle, averaged error reduction rates

disc.	mesh level						
	2	3	4	5	6	7	8
Q_2/Q_1	4.63e-2	5.86e-2	7.54e-2	6.15e-2	6.09e-2	5.66e-2	5.32e-2
Q_2/P_1^{disc}	7.03e-2	6.27e-2	7.91e-2	6.94e-2	6.61e-2	6.21e-2	5.85e-2
P_2/P_1	9.66e-2	1.76e-1	1.62e-1	1.59e-1	1.55e-1	1.49e-1	1.43e-1
Q_3/Q_2	1.27e-1	1.49e-1	1.33e-1	1.42e-1	1.32e-1	1.26e-1	
Q_3/P_2^{disc}	1.32e-1	1.39e-1	1.33e-1	1.25e-1	1.19e-1	1.13e-1	
P_3/P_2	2.88e-1	4.02e-1	3.99e-1	4.19e-1	3.99e-1	3.95e-1	
Q_4/Q_3	4.82e-1	4.80e-1	4.73e-1	4.66e-1	4.59e-1		
Q_4/P_3^{disc}	2.29e-1	2.27e-1	2.25e-1	2.21e-1	2.18e-1		

Although system (11) is solved only approximately in each smoothing step, the results in Table 5 show averaged error reduction rates which are independent of the level.

Example 4.4. *W-cycle in a 3d test case*. This example demonstrates the behaviour of the multi-level solver applied to a three-dimensional problem. We consider $\Omega = (0,1)^3$ with the prescribed solution $u = (u_1, u_2, u_3)$ and p given by

$$
\begin{aligned}
u_1(x,y,z) &= \sin(\pi x)\sin(\pi y)\sin(\pi z) + x^4\cos(\pi y),\\
u_2(x,y,z) &= \cos(\pi x)\cos(\pi y)\cos(\pi z) - 3y^3 z,\\
u_3(x,y,z) &= \cos(\pi x)\sin(\pi y)\cos(\pi z) + \cos(\pi x)\sin(\pi y)\sin(\pi z)\\
&\quad - 4x^3 z\cos(\pi y) + 4.5y^2 z^2,\\
p(x,y,z) &= 3x - \sin(y+4z) + c.
\end{aligned}
$$

The constant c is chosen such that $p \in L_0^2(\Omega)$ and the right hand side f is chosen such that (u,p) fulfil (3).

For discretisations based on hexahedra, the initial grid (level 0) was obtained by dividing the unit cube into eight cubes of edge length $1/2$ as indicated in Fig. 5. The initial grid for discretisations based on simplicial mesh cells consists of 48 tetrahedra. The corresponding numbers of degrees of freedom are given in

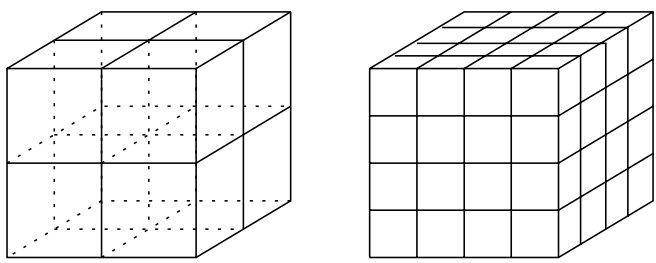

Figure 5. Mesh level 0 (left) and 1 (right)

Table 6. Degrees of freedom for the discretisations in the 3d test case, Example 4.4

disc.	mesh level					
	1	2	3	4	5	6
Q_1^{rot}/Q_0	116	784	5696	43264	336896	2658304
P_1^{nc}/P_0	408	2976	22656	176640	1394688	11083776
Q_2/Q_1	402	2312	15468	112724	859812	6714692
Q_2/P_1^{disc}	407	2443	16787	124195	954947	7488643
P_2/P_1	402	2312	15468	112724	859812	6714692
Q_3/Q_2	1154	7320	51788	388884	3012644	
Q_3/P_2^{disc}	1109	7231	51995	393907	3065699	
P_3/P_2	1154	7320	51788	388884	3012644	

Table 7. Example 4.4, $D_l = ILU(A_l)$, $\alpha_l = 1.5$, $W(3,3)$-cycle, averaged error reduction rate

disc.	mesh level				
	2	3	4	5	6
Q_2/Q_1	8.11e-3	3.14e-2	4.08e-2	3.83e-2	3.23e-2
Q_2/P_1^{disc}	7.14e-3	3.14e-2	3.97e-2	3.59e-2	3.50e-2
P_2/P_1	4.28e-2	7.12e-2	6.79e-2	6.90e-2	7.00e-2
Q_3/Q_2	3.78e-2	7.89e-2	8.37e-2	7.26e-2	
Q_3/P_2^{disc}	3.71e-2	7.80e-2	8.16e-2	7.16e-2	
P_3/P_2	6.24e-2	8.85e-2	8.57e-2	7.72e-2	

Table 6. It is noteworthy that sometimes a lower order finite element space possesses more degrees of freedom than a higher order space on the same mesh level, e.g. compare P_1^{nc}/P_0 and P_2/P_1.

Table 7 presents results obtained with the $W(3,3)$-cycle, $D_l = ILU(A_l)$ and $\alpha_l = 1.5$. The saddle point problems in the smoothing process (11) were solved up to a reduction of the Euclidean norm of the residual by a factor 10^4 or at most 20 flexible GMRES iterations. Computations with weaker stopping criteria did not lead to such clearly level-independent rates of convergence as presented in Table 7. This behaviour corresponds to the theory by Zulehner [36] which is valid if the approximation of the solution of (11) is close enough to the solution.

Acknowledgements

The research of Petr Knobloch has been supported under the grants No. 201/99/P029 and 201/99/0267 of the Czech Grant Agency and by the grant MSM 113200007. The research of Gunar Matthies has been partially supported under the grant FOR 301 of the DFG.

References

[1] Bank, R. E., Welfert, B. D., Yserentant, H.: A class of iterative methods for solving saddle point problems. Numer. Math. *56*, 645–666 (1990).
[2] Bernardi, C., Raugel, G.: Analysis of some finite elements for the Stokes problem. Math. Comp. *44*, 71–79 (1985).
[3] Braess, D., Dahmen, W., Wieners, C.: A multigrid algorithm for the mortar finite element method. SIAM J. Numer. Anal. *37*, 48–69 (1999).

[4] Braess, D., Dryja, M., Hackbusch, W.: A multigrid method for nonconforming fe-discretisations with applications to non-matching grids. Computing *63*, 1–25 (1999).
[5] Braess, D., Sarazin, R.: An efficient smoother for the Stokes problem. Appl. Numer. Math. *23*, 3–19 (1997).
[6] Braess, D., Verfürth, R.: Multigrid methods for nonconforming finite element methods. SIAM J. Numer. Anal. *27*, 979–986 (1990).
[7] Bramble, J. H.: Multigrid Methods. Pitman Research Notes in Math, vol. 294. London: Longman, 1993.
[8] Brenner, S. C.: An optimal-order multigrid method for P_1 nonconforming finite elements. Math. Comp. *52*, 1–15 (1989).
[9] Brenner, S. C.: A nonconforming multigrid method for the stationary Stokes equations. Math. Comp. *55*, 411–437 (1990).
[10] Brenner, S. C.: Convergence of nonconforming multigrid methods without full elliptic regularity. Math. Comp. *68*, 25–53 (1999).
[11] Chen, Z.: On the convergence of Galerkin-multigrid methods for nonconforming finite elements. East-West J. Numer. Math. *7*, 79–104 (1999).
[12] Chen, Z.: On the convergence of nonnested multigrid methods with nested spaces on coarse grids. Numer. Methods in Partial Differential Equations *16*, 265–284 (2000).
[13] Chen, Z., Kwak, D. Y.: Multigrid algorithms for the nonconforming and mixed methods for nonsymmetric and indefinite problems. SIAM J. Sci. Comput. *19*, 502–515 (1998).
[14] Chen, Z., Oswald, P.: Multigrid and multilevel methods for nonconforming Q_1 elements. Math. Comput. *67*, 667–693 (1998).
[15] Ciarlet, P. G.: The finite element method for elliptic problems. Studies in Mathematics and its Applications, vol. 4. Amsterdam, New York, Oxford: North-Holland, 1978.
[16] Crouzeix, M., Raviart, P.-A.: Conforming and nonconforming finite element methods for solving the stationary Stokes equations I. RAIRO. Analyse Numérique *7*, 33–76 (1973).
[17] Girault, V., Raviart, P.-A.: Finite element methods for Navier–Stokes equations. Berlin: Springer, 1986.
[18] Hackbusch, W.: Multi-grid methods and applications. Number 4 in SCM. Berlin: Springer, 1985.
[19] John, V.: Higher order finite element methods and multigrid solvers in a benchmark problem for the 3d Navier–Stokes equations. Preprint 01-18, Fakultät für Mathematik, Otto-von-Guericke-Universität Magdeburg, 2001.
[20] John, V., Matthies, G.: Higher order finite element discretizations in a benchmark problem for incompressible flows. Int. J. Numer. Methods Fluids *37*, 885–903 (2001).
[21] John, V., Tobiska, L.: A coupled multigrid method for nonconforming finite element discretizations of the Stokes equation. Computing *64*, 307–321 (2000).
[22] John, V., Tobiska, L.: Numerical performance of smoothers in coupled multigrid methods for the parallel solution of the incompressible Navier–Stokes equations. Int. J. Numer. Meth. Fluids *33*, 453–473 (2000).
[23] Knobloch, P.: On Korn's inequality for nonconforming finite elements. Techn. Mech. *20*, 205–214 and 375 (errata) (2000).
[24] Knobloch, P.: On the inf-sup condition for the P_1^{mod} element. Preprint No. MATH-KNM-2001/4, Faculty of Mathematics and Physics, Charles University, Prague, 2001.
[25] Knobloch, P., Tobiska, L.: The P_1^{mod} element: A new nonconforming finite element for convection diffusion problems. Preprint 99-28, Fakultät für Mathematik, Otto-von-Guericke-Universität Magdeburg, 1999.
[26] Rannacher, R., Turek, S.: Simple nonconforming quadrilateral Stokes element. Numer. Methods Partial Differential Equations *8*, 97–111 (1992).
[27] Saad, Y.: A flexible inner-outer preconditioned GMRES algorithm. SIAM J. Sci. Comput. *14*, 461–469 (1993).
[28] Saad, Y., Schultz. M. H.: GMRES: A generalized minimal residual algorithm for solving nonsymmetric linear systems. SIAM J. Sci. Stat. Comput. *7*, 856–869 (1986).
[29] Sarazin, R.: Eine Klasse von effizienten Glättern vom Jacobi-Typ für das Stokes-Problem. PhD Thesis, Ruhr-Universität Bochum, 1996.
[30] Schieweck, F.: Parallele Lösung der stationären inkompressiblen Navier-Stokes-Gleichungen. Habilitationsschrift, Otto-von-Guericke-Universität Magdeburg, 1997. To be downloaded from: http://david.math.uni-magdeburg.de/home/schieweck.
[31] Schieweck, F.: A general transfer operator for arbitrary finite element spaces. Preprint 00-25, Fakultät für Mathematik, Otto-von-Guericke-Universität Magdeburg, 2000.
[32] Shaidurov, V. V.: Multigrid Methods for Finite Elements. New York: Kluwer, 1989.

[33] Turek, S.: Multigrid techniques for a divergence-free finite element discretization. East-West J. Numer. Math. *2*, 229–255 (1994).
[34] Turek, S.: Efficient solvers for incompressible flow problems. Number 6 in Lect. Notes Comput. Sci. Engrg. Berlin, Heidelberg, New York, Tokyo: Springer, 1999.
[35] Ye, X., Anderson, G.: The derivation of minimal support basis functions for the discrete divergence operator. J. Comput. Appl. Math. *61*, 105–116 (1995).
[36] Zulehner, W.: A class of smoothers for saddle point problems. Computing *65*, 227–246 (2000).

V. John
G. Matthies
L. Tobiska
Institut für Analysis und Numerik
Otto-von-Guericke-Universität Magdeburg
PF 4120, D-39016 Magdeburg
Germany
e-mails: john@mathematik.uni-magdeburg.de
matthies@mathematik.uni-magdeburg.de
tobiska@mathematik.uni-magdeburg.de

P. Knobloch
Institute of Numerical Mathematics
Faculty of Mathematics and Physics
Charles University
Sokolovská 83, 186 75 Praha 8
Czech Republic
e-mail: knobloch@karlin.mff.cuni.cz